

## Theoretical and experimental study of triphenylphosphonium Schiff base of 5-hydroxy-3-methyl-1-phenyl-4-formylpyrazole

Sergey A. Borodkin, Leonid D. Popov, Arshak A. Tsaturyan, Milica R. Milenković, Igor N. Shcherbakov & Vladimir V. Lukov

To cite this article: Sergey A. Borodkin, Leonid D. Popov, Arshak A. Tsaturyan, Milica R. Milenković, Igor N. Shcherbakov & Vladimir V. Lukov (2018): Theoretical and experimental study of triphenylphosphonium Schiff base of 5-hydroxy-3-methyl-1-phenyl-4-formylpyrazole, Phosphorus, Sulfur, and Silicon and the Related Elements, DOI: [10.1080/10426507.2018.1424159](https://doi.org/10.1080/10426507.2018.1424159)

To link to this article: <https://doi.org/10.1080/10426507.2018.1424159>

 View supplementary material 

 Accepted author version posted online: 05 Jan 2018.

 Submit your article to this journal 

 View related articles 

 View Crossmark data 

## Theoretical and experimental study of triphenylphosphonium Schiff base of 5-hydroxy-3-methyl-1-phenyl-4-formylpyrazole

Sergey A. Borodkin<sup>a</sup>, Leonid D. Popov<sup>a</sup>, Arshak A. Tsaturyan<sup>a</sup>, Milica R. Milenković<sup>b</sup>, Igor N. Shcherbakov<sup>a</sup>, Vladimir V. Lukov<sup>a</sup>

<sup>a</sup> *Chemistry Department Southern Federal University, 344090, Rostov-on-Don, Russia, Zorge St., 7*

<sup>b</sup> *Faculty of Chemistry, University of Belgrade, Studentski trg 12-16, Belgrade, Serbia*

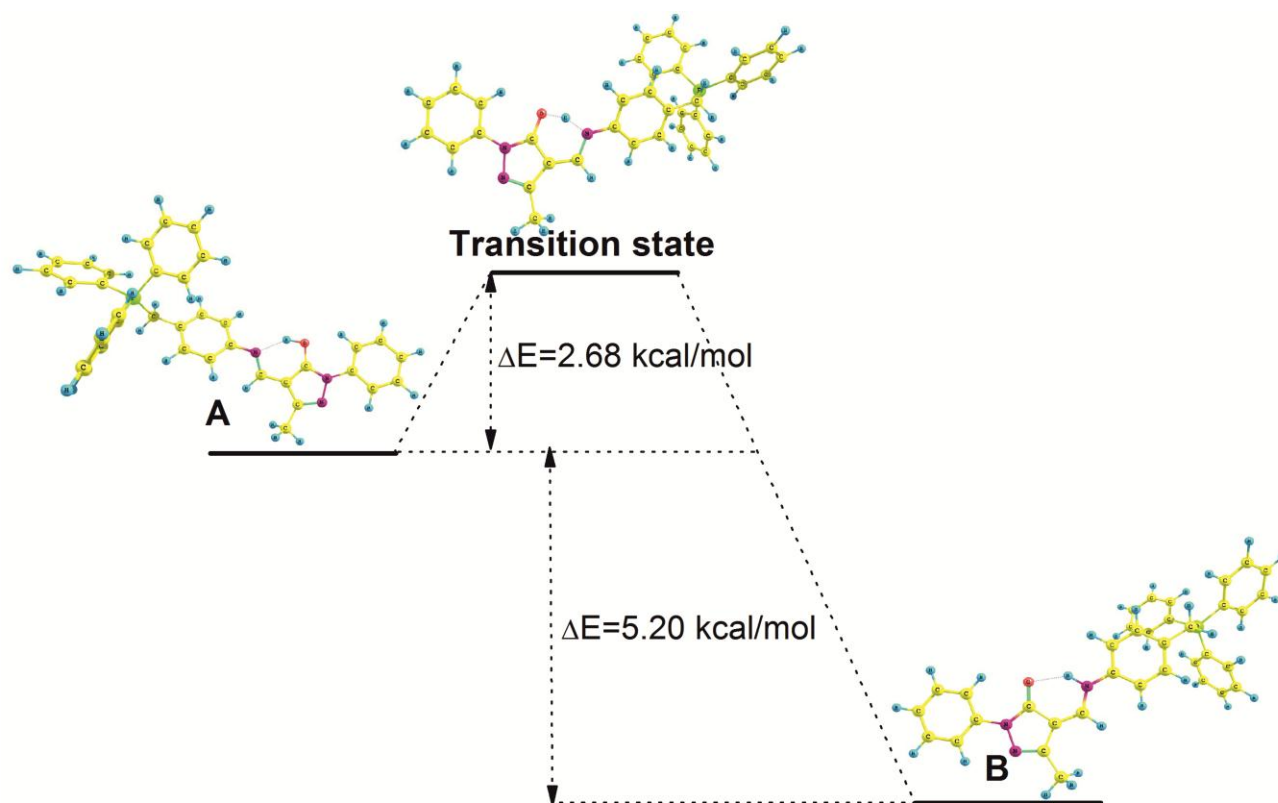
Email: [caturyan@sfedu.ru](mailto:caturyan@sfedu.ru)

### *Abstract*

The Schiff base (**HLBr**), containing a chelating unit and triphenylphosphonium moiety has been synthesized in the reaction of 4-aminobenzyl(triphenyl)phosphonium bromide with 5-hydroxy-3-methyl-1-phenyl-4-formylpyrazole. The composition and structure of **HLBr** have been determined by elemental analysis, IR, 1D and 2D NMR, electronic spectroscopy and mass spectrometry. Density functional theory (DFT) calculations (6-311G(d,p) level of theory) have been carried out to investigate tautomeric forms of **HL**<sup>+</sup> and the reaction mechanism of its formation and spectral properties. The most stable form in the solid state and in DMSO solution is pyrazolone (keto-amine) tautomeric form.

Keywords: Schiff base, tautomerism, phosphonium salts, quantum-chemical calculations.

Graphical Abstract



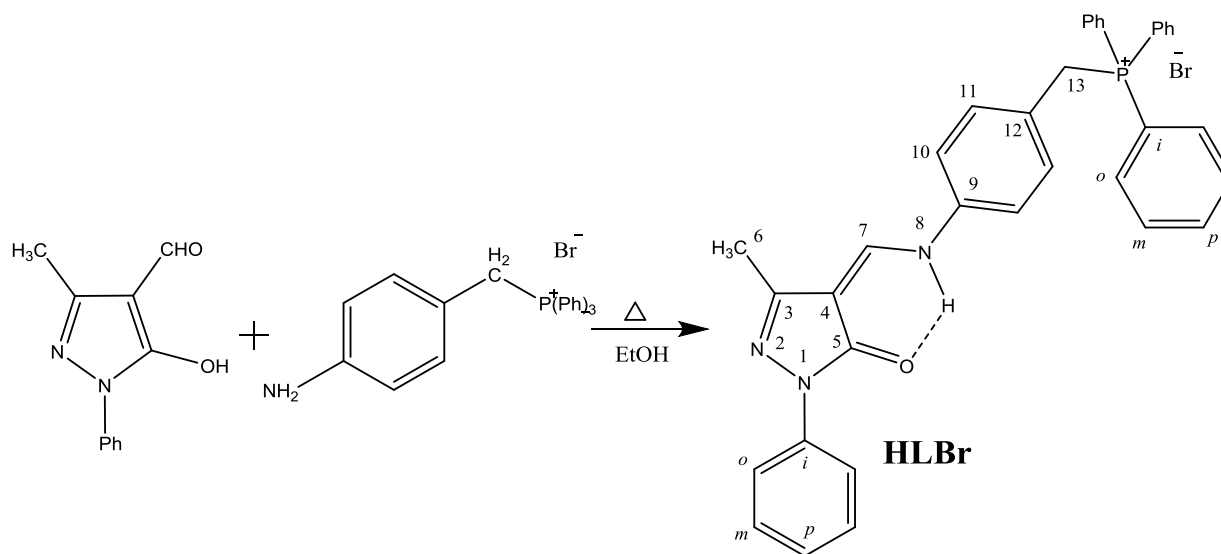
## 1. Introduction

Quaternary phosphonium salts have been of interest due to their various application as reagents, green solvents and new materials [1–3]. Also, cationic lipophilic salts containing a quaternary phosphonium group can be used as carriers for mitochondria-targeted drugs with a high preference towards tumor cells and cardiac muscle cells [4–6]. Phosphonium salts are easily accessible and frequently used intermediates in organic synthesis, long known phase-transfer catalysts and potential Lewis acid organocatalysts [7]. Pyrazolone derivatives are intensively investigated, because of their interesting structural properties and applications in diverse areas [8–13]. Among pyrazol-5-one derivatives, 4-acyl pyrazolones, have attracted considerable attention due to their biological activities, photochromic properties and applications in catalysis and analytical chemistry. Also, this class of compounds and their corresponding Schiff bases possess interesting coordination properties [14–21]. The combination of positively charged phosphonium group with chelatofore pyrazolone moiety can result in a promising ligand system leading to coordination compounds with enhanced solubility, tunable redox properties and biological activity. This work is devoted to the study of a cationic chelator (**HLBr**) synthesized in the condensation reaction between 4-aminobenzyl(triphenyl)phosphonium bromide and 5-hydroxy-3-methyl-1-phenyl-4-formylpyrazole.

## 2. Results and discussion

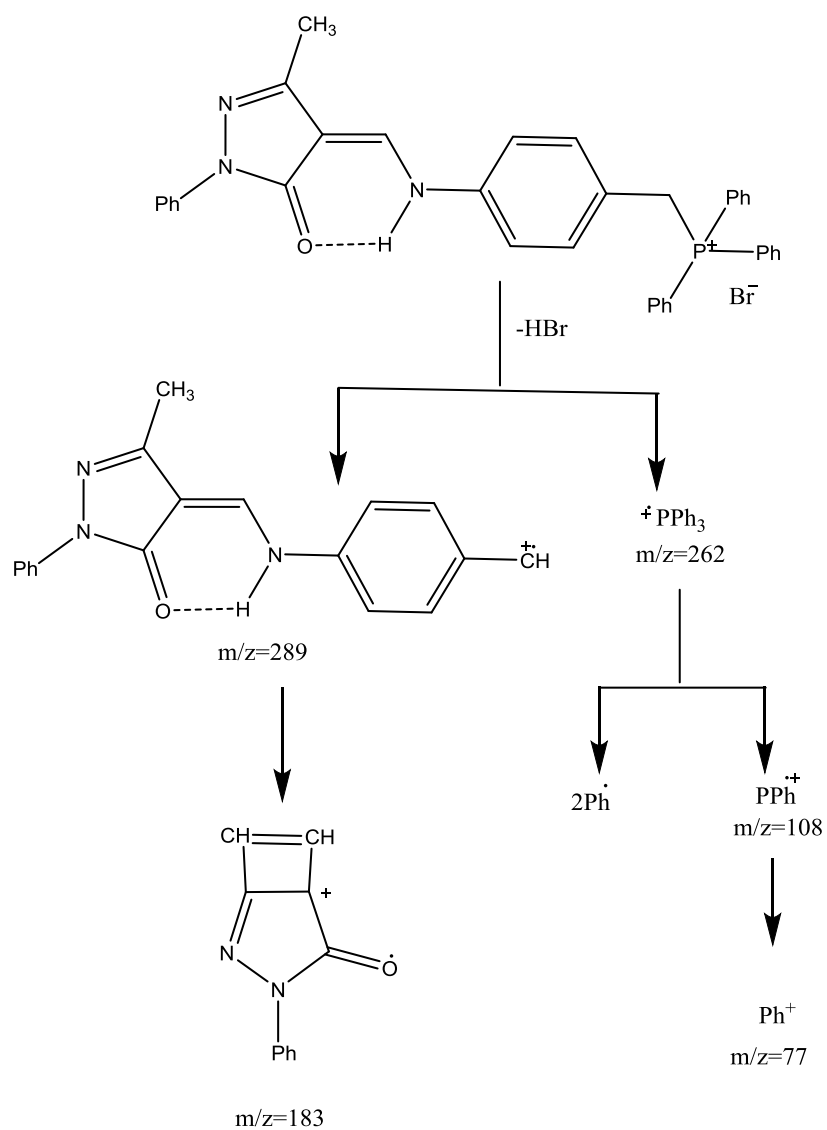
### 2.1. Synthesis of **HLBr**

The phosphonium azomethine (**HLBr**) was prepared by refluxing of the ethanolic solution of equivalent amounts of 4-aminobenzyl(triphenyl)phosphonium bromide and 5-hydroxy-3-methyl-1-phenyl-4-formylpyrazole (Scheme 1).

Scheme 1. The synthesis of **HLBr**

*2.2. Mass-spectrum of HLBr*

Molecular ion peak ( $m/z = 631$ ) was not registered in the mass spectrum of **HLBr**. The two intensive peaks with  $m/z=262$  (100) corresponding to  $\text{Ph}_3\text{P}^+$  ion and  $m/z=183$  (99) and three peaks with lower intensity  $m/z=108$  (60),  $m/z = 77$  (40) and  $m/z=289$  (34) have been observed in the mass spectrum of **HLBr**. The data allows us to suggest mechanism for **HLBr** fragmentation under the electron impact ionization which is shown in Scheme 2.



Scheme 2. The proposed mechanism of **HLBr** fragmentation under electron impact ionization.

### 2.3 NMR, IR and UV/Vis spectroscopy study

Chemical shifts of individual atoms were assigned (see Synthesis section for results and Scheme 1 for atom numbering) according to 1D ( $^1\text{H}$ ,  $^{13}\text{C}$ ,  $^{15}\text{N}$  and  $^{31}\text{P}$ ) and 2D COSY ( $^1\text{H}$ - $^1\text{H}$ ), NOESY( $^1\text{H}$ - $^1\text{H}$ ), HSQC( $^1\text{H}$ - $^{13}\text{C}$ ), and HMBC ( $^1\text{H}$ - $^{13}\text{C}$ ,  $^1\text{H}$ - $^{15}\text{N}$ ) NMR experiments (experimental spectra are shown in Figures S 2-S 9 of the Supplemental Materials). The complete assignment of the signals in the  $^1\text{H}$  NMR spectra is the following ( $\delta$ , ppm): the signal of pyrazolone moiety  $\text{CH}_3$  group is registered as singlet at 2.25 ppm, the signal of the  $\text{CH}_2$  group protons form a doublet due to spin-coupling with phosphorus nucleus at 5.20 ppm with  $^2J_{\text{PH}} = 15.4$  Hz. Signals of phenyl groups protons in *ortho*-, *meta*- and *para*-positions are found as three complex multiplets in the ranges 7.66-7.71 (6H intensity), 7.73-7.79 (6H) and 7.88-7.93 (3H), correspondingly. Spin-coupled protons of N-benzyl moiety ( $^3J_{\text{HH}} = 8.7$  Hz) appear in spectra as two doublet signals with two-proton intensity at 7.02 ( $\text{H}^{11}$ ) and 7.45 ppm ( $\text{H}^{10}$ ), former is additionally splitted due to interaction with phosphorous nucleus ( $^4J_{\text{PH}} = 2.54$  Hz). *Ortho*-, *meta*- and *para*-proton signals of N-phenyl substituent in pyrazolone moiety are found at 7.95 (d, 2H,  $^3J_{\text{HH}} = 8.6$  Hz), 7.37 (dd, 2H,  $^3J_{\text{HH}} = 7.4$ ,  $^3J_{\text{HH}} = 8.6$  Hz) and 7.11 ppm (t, 1H,  $^3J_{\text{HH}} = 7.4$  Hz), correspondingly. The signal of  $\text{H}^7$  proton of 1H intensity is registered as broadened singlet at 8.51 ppm, even more broadened is the singlet signal of  $\text{D}_2\text{O}$  exchangeable NH proton at 11.22 ppm. Location of the proton on  $\text{N}^8$  nitrogen atom is supported by the presence of cross-peak in COSY  $^1\text{H}$  spectrum at (8.51, 11.22) ppm due to spin coupling  $\text{H}^7 - \text{H}^8$ . Absence of distinct splitting of the NH and  $\text{CH}^7$  signals in 1D  $^1\text{H}$  spectrum can be attributed to fast exchange of the

NH proton with residual water in DMSO solvent, which is supported by presence of strong NOESY  $^1\text{H}$  cross-peak at (3.32, 11.22) ppm.

Signals in  $^{13}\text{C}$  NMR spectrum are readily assigned, especially in arylphosphonium moiety due to characteristic spin coupling with  $^{31}\text{P}$  nucleus resulting in doublet-shape signals. The greatest coupling  $^1J_{PC} = 85.5$  Hz is observed for signals of the closest phenyl substituents carbon atoms (117.7 ppm) and  $^1J_{PC} = 46.5$  Hz for methylene carbon atom (27.8 ppm). Carbon atoms of P-phenyl substituents in *ortho*-, *meta*- and *para*-positions are observed at 134.0 ( $^2J_{PC} = 9.9$  Hz), 130.1 ( $^3J_{PC} = 12.4$  Hz) and 135.1 ppm ( $^4J_{PC} = 3.0$  Hz), correspondingly. Doublet signals at 124.3 ( $^2J_{PC} = 8.8$  Hz), 131.9 ( $^3J_{PC} = 5.6$  Hz), 117.9 ( $^4J_{PC} = 3.3$  Hz) and 138.7 ( $^5J_{PC} = 4.0$  Hz) are assigned to N-benzyl moiety carbon atoms  $\text{C}^{12}$ ,  $\text{C}^{11}$ ,  $\text{C}^{10}$  and  $\text{C}^9$ , respectively. Singlet signals are assigned with the help of 2D HSQC and HMBC  $^1\text{H}$ - $^{13}\text{C}$  NMR techniques. N-Phenyl substituent carbon atom signals are assigned as following: 138.9 (*i*-NPh), 117.5 (*o*-NPh), 128.7 (*m*-NPh) and 123.8 ppm (*p*-NPh). Pyrazolone ring carbons  $\text{C}^5$  and  $\text{C}^3$  are substantially deshielded (164.7 and 149.0 ppm, correspondingly) relative to  $\text{C}^4$  one (102.2 ppm). Formyl and, methyl groups carbon signals are found at 145.2 and 12.6 ppm, respectively.

In  $^{15}\text{N}$  NMR spectrum three signals are observed at -92.4 ( $\text{N}^2$ ), -190.9 ( $\text{N}^1$ ), -252.5 ppm ( $\text{N}^8$ ). In  $^1\text{H}$ - $^{15}\text{N}$  HMBC spectra the following cross-peaks were found:  $\text{N}^2$ -methyl group protons,  $\text{N}^1$  - *ortho*- and  $\text{N}^1$  - *meta*-protons of N-phenyl substituent and weak signal corresponding to  $\text{N}^1$  - methyl group protons interaction. For nitrogen atom  $\text{N}^8$  cross-peak was registered only with  $\text{C}^{10}$ -H protons.

Thus, based on NMR data we can conclude that  $\text{HL}^+$  exists in DMSO solution in keto-amine tautomeric form.

Assignment of the absorption bands in IR spectrum was made by comparison of the simulated (at the B3LYP/6-311G(d,p) level of theory) and experimental spectrum (see Table 1).

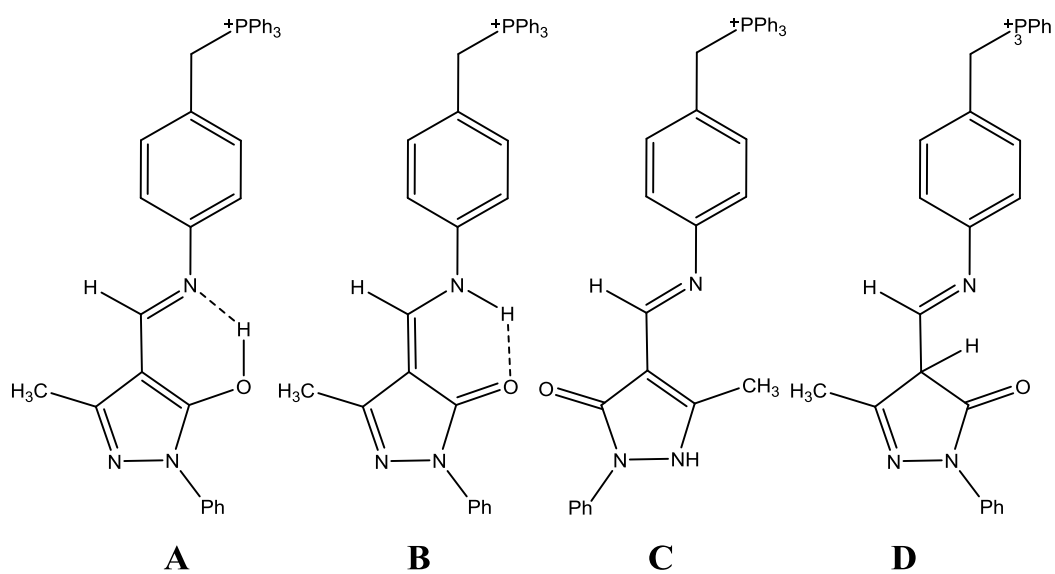
**Table 1.** The calculated and experimental IR spectroscopy data for **HLBr**

| Type of vibration                                       | Experiment, $\text{cm}^{-1}$ | Calculation              |           |
|---|------------------------------|--------------------------|-----------|
|   |                              | $\nu$ , $\text{cm}^{-1}$ | Intensity |
| $\nu(\text{NH})$  | 3300-3450 (br)               | 3181                     | 212.2     |
| $\nu(\text{CH})$ arom                                   | 2975-3105 (w)                | 3028-3132                | 0.5-28.1  |
| $\nu(\text{CH}_2)$                                      | 2885 (w)                     | 2971                     | 15.3      |
| $\nu(\text{CH}_3)$                                      | 2857 (w)                     | 2954                     | 12.4      |
| $\nu(\text{C}(\text{O})-\text{C}=\text{C})_{\text{as}}$ | 1650 (s)                     | 1660                     | 1036      |
| $\nu(\text{C}(\text{O})-\text{C}=\text{C})_{\text{s}}$  | 1623 (m)                     | 1639                     | 235       |
| $\nu(\text{C}=\text{C})$ aminobenzyl                    | 1596 (m)                     | 1597                     | 444.5     |
| $\delta(\text{NH})$                                     | 1488 (m)                     | 1477                     | 320       |
| $\nu(\text{C}=\text{C})$ P <sup>+</sup> -Ph             | 1440 (m)                     | 1422-1424                | 76        |
| $\nu(\text{C}-\text{N})$                                | 1291 (s)                     | 1275                     | 1015      |
| $\nu(\text{P}^+-\text{C})$                              | 1113 (m, broadened)          | 1075-1079                | 11.8-58.3 |

The broad band at  $3300\text{ cm}^{-1}$  in the IR spectrum of azomethine **HL**Br can be attributed to stretching vibrations of intramolecular H-bonded NH group. Weak absorption bands in the region  $3028\text{-}3132\text{ cm}^{-1}$  are due to numerous C-H stretching vibrations of aromatic rings, while aliphatic C-H stretching vibrations of methylene and methyl groups are found at  $2885$  and  $2857\text{ cm}^{-1}$ , correspondingly. Delocalized antisymmetric and symmetric stretching vibrations with major contribution of conjugated carbonyl and C=C exocyclic double bonds of pyrazolone moiety are found at  $1650$  and  $1623\text{ cm}^{-1}$ , respectively. Medium strength absorption at  $1596\text{ cm}^{-1}$  is due to the C=C para-substituted aromatic ring stretching vibration of the aminobenzyl moiety. Deformation vibration of NH group appears as a medium strength band at  $1488\text{ cm}^{-1}$ . Medium intensity bands at  $1113\text{ cm}^{-1}$  and  $1440\text{ cm}^{-1}$  are characteristic for triphenylphosphonium salts and correspond to  $\text{P}^+\text{-C}$  stretching and P-phenyl rings skeleton vibrations, correspondingly. IR data also supports the proposal that in solid sample pyrazolone tautomeric form is present, due to satisfactory correspondence between experimental and calculated vibrational spectrum of the isomers.

#### 2.4. Quantum-chemical study of **HL**<sup>+</sup> tautomeric forms

It is well-known that 5-hydroxy-4-formyl-pyrazol azomethine derivatives can exist in different prototropic tautomeric forms [22]. Quantum-chemical calculations have been carried out in order to estimate the relative stability of the tautomers and the most stable tautomeric forms **A** - **D** according to calculations of **HL**<sup>+</sup> are shown in Scheme 3.

Scheme 3. The most stable tautomeric forms of **HL**<sup>+</sup>.

The calculated total energies and relative stabilities ( $\Delta E$ , kcal/mol) for the modeled tautomeric forms of **HL**<sup>+</sup> are shown in Table 2.

**Table 2.** The quantum-chemical calculation data for the most stable tautomeric forms **A** – **D** of **HL**<sup>+</sup> (total ( $E$ , a.u.) and relative ( $\Delta E$ , kcal/mol) energies, B3LYP/6-311G(d,p))

| Structure | gas phase        |                          | DMSO             |                          | CHCl <sub>3</sub> |                          |
|-----------|------------------|--------------------------|------------------|--------------------------|-------------------|--------------------------|
|           | $E$ , a.u.       | $\Delta E$ ,<br>kcal/mol | $E$ , a.u.       | $\Delta E$ ,<br>kcal/mol | $E$ , a.u.        | $\Delta E$ ,<br>kcal/mol |
| <b>A</b>  | -<br>1971.546742 | 5.20                     | -<br>1971.607891 | 10.12                    | -<br>1971.594127  | 8.77                     |
| <b>B</b>  | -<br>1971.555029 | 0.00                     | -<br>1971.624018 | 0.00                     | -<br>1971.608098  | 0.00                     |
| <b>C</b>  | -<br>1971.536195 | 11.82                    | -<br>1971.601747 | 13.98                    | -<br>1971.586577  | 13.50                    |
| <b>D</b>  | -<br>1971.524898 | 18.91                    | -<br>1971.589989 | 21.35                    | -<br>1971.575427  | 20.50                    |

The results of quantum-chemical calculations showed that the most stable form of  $\mathbf{HL}^+$  in gaseous phase is the keto-amine (pyrazolone) form **B** stabilized by intramolecular H-bonding between NH group and oxygen atom of pyrazolone moiety. The enol-imine (5-hydroxypyrazole) form **A**, with  $\text{OH}\cdots\text{N}$  intramolecular H-bonding is 5.2 kcal/mol less stable relative to form **B**. The keto-imine tautomers (**C** and **D**) are 11.82–18.91 kcal/mol destabilized relative to the **B** isomer. The data of quantum-chemical modeling of  $\mathbf{HL}^+$  tautomers in solvents within PCM approximation show the growth of the relative stability of the **B** tautomer both in DMSO and  $\text{CHCl}_3$  media, especially noticeable for **A** isomer which is nearly twice destabilized relative to **B** in the solution compared to gaseous phase. These results are in line with experimental NMR and IR data, evidencing both in DMSO solution and in solid phase formation of the pyrazolone tautomeric form.

### 2.5. Intramolecular proton transfer $\mathbf{HL}^+$ in gas phase

Since the compound  $\mathbf{HL}^+$  is obtained in the condensation reaction of 4-aminobenzyl(triphenyl)phosphonium bromide and 5-hydroxy-3-methyl-1-phenyl-4-formylpyrazole, the first stage of the most probable mechanism of this reaction includes the formation of **A** tautomer (kinetic product) followed by its transformation into the thermodynamically preferred form **B**. The latter is taking place through 1-5 sigmatropic shift of proton of hydroxypyrazole fragment. This rearrangement is carried out through the transition state shown in Figure 1.

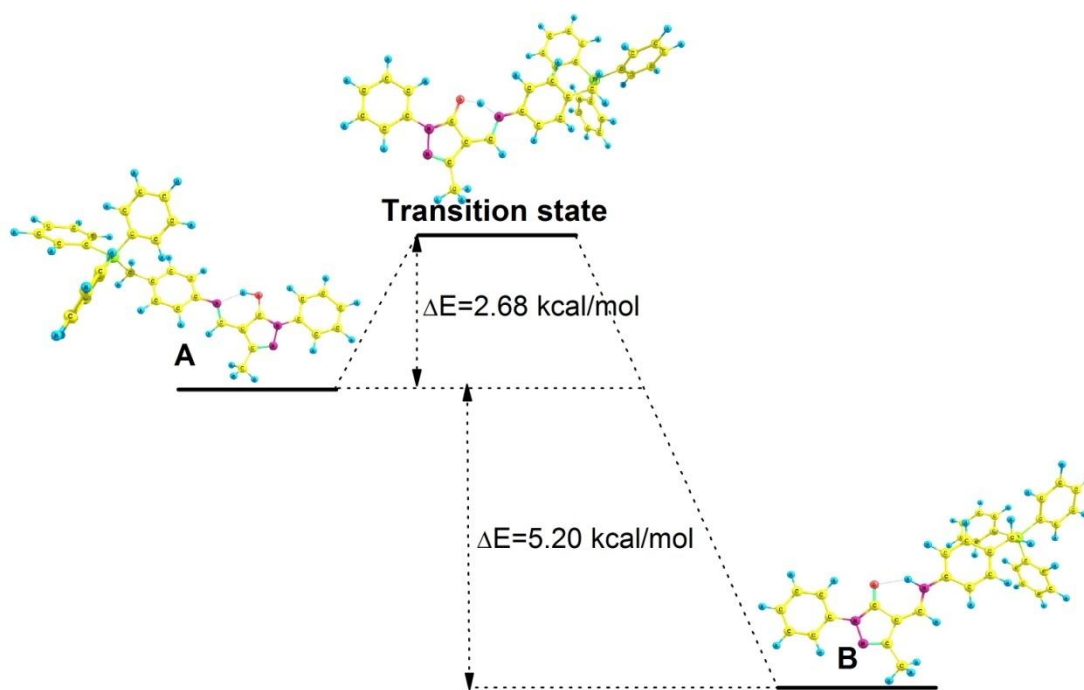


Figure 1. Energy diagram of tautomeric proton shift leading from **A** to **B** isomer

The calculated activation energy of this process in gas phase is only 2.68 kcal/mol so kinetic enol-imine product **A** will readily convert to thermodynamically most stable keto-amine **B** tautomer.

### 2.6. Electronic spectra

In UV/vis spectra of **HLBr** ethanolic solution (Figure 2, solid curve) the absorption bands at  $\lambda_{\max} = 346$  nm ( $\lg \epsilon_{\max} = 4.37$ ), 198 nm ( $\lg \epsilon_{\max} = 4.38$ ) and shoulder at 226 ( $\lg \epsilon_{\max} = 3.91$ ) – 256 ( $\lg \epsilon_{\max} = 3.62$ ) nm are registered. Changes in pH of solution do not exert essential influence on **HLBr** electronic spectrum, the longwave band shifts to  $\lambda_{\max} = 350$  nm ( $\lg \epsilon_{\max} = 4.32$ ) after the addition of triethylamine and to  $\lambda_{\max} = 350$  nm ( $\lg \epsilon_{\max} = 4.13$ ) when HCl was added. The performed quantum chemical modelling of UV/vis spectrum of tautomeric form **B** within TDDFT approximation (6-311G(d,p)) revealed that the longwave absorption band arises mainly from the electron transition from HOMO-1 to LUMO (Table 3).

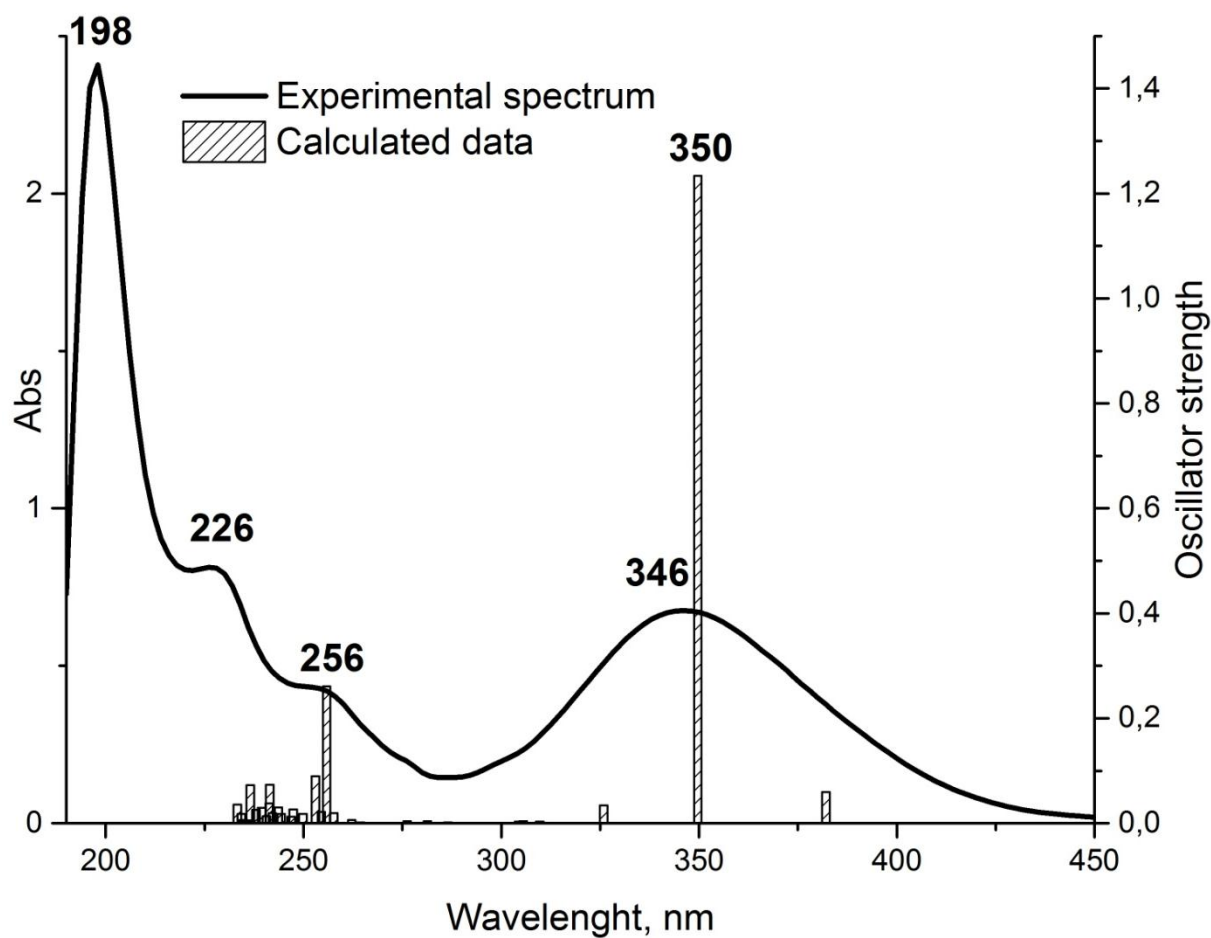


Figure 2. Experimental (ethanol solution, solid line) and calculated (vertical lines) UV/vis spectrum of **HLBr**

In Figure 2 the calculated transition wavelengths are shown as black vertical lines. The calculated excitation wavelength (350 nm) is in excellent agreement with experimental result. Also close to experiment is the calculated wavelength of the transition appearing as a shoulder at 256 nm.

**Table 3.** The vertical singlet excitations characteristics for  $\mathbf{HL}^+$ : number of the excited states, transition composition, excitation energy (eV), wavelength (nm), oscillator strength (TDDFT,

6-311G(d,p))

| Excited State | Transition (contrib. %)  | $\Delta E$ , eV | $\lambda$ , nm | f (oscillator strength) |
|---------------|--|-----------------|----------------|-------------------------|
| 2             | HOMO-1 $\rightarrow$ LUMO (77%)<br>HOMO $\rightarrow$ LUMO (8%)    | 3.55            | 350            | 1.2335                  |
| 17            | HOMO-4 $\rightarrow$ LUMO (11%)<br>HOMO $\rightarrow$ LUMO+8 (49%) | 4.85            | 256            | 0.2607                  |

HOMO-1, HOMO and LUMO are of  $\pi$ -type so the longwave transitions are of  $\pi$ - $\pi^*$  character (for the shapes of the frontier molecular orbitals see Figure S1 in Supplemental Materials). Large value of oscillator strength of the transition at 350 nm is due to localization of HOMO-1 and LUMO on different moieties of  $\pi$ -conjugated bond system.

A theoretical study of vertical excitation energies for deprotonated form of the compound, **L**, revealed an insignificant long-wave shift of the adsorption band coinciding well with the experimental observations.

### 3. Experimental

#### 3.1. Reagents

Triphenylphosphine and 1-phenyl-3-methyl-2-pyrazolin-5-one were purchased from Aldrich. All solvents were purified with standard methods before usage.

#### 3.2. Instruments

Mass spectra of **HLBr** were measured with Finnigan MAT INCOS 50 instrument (electron impact, 70 eV).  $^1\text{H}$ ,  $^{13}\text{C}$ ,  $^{15}\text{N}$ ,  $^{31}\text{P}$  NMR, the 2D spectra of  $^1\text{H}$ - $^1\text{H}$  COSY,  $^1\text{H}$ - $^1\text{H}$  NOESY,  $^1\text{H}$ - $^{13}\text{C}$  HSQC,  $^1\text{H}$ - $^{13}\text{C}$ ,  $^1\text{H}$ - $^{15}\text{N}$ ,  $^1\text{H}$ - $^{31}\text{P}$  HMBC spectra were measured on a Bruker Avance-600 spectrometer at 600 ( $^1\text{H}$ ), 151 ( $^{13}\text{C}$ ), 60 ( $^{15}\text{N}$ ) or 243 MHz ( $^{31}\text{P}$ ), using DMSO- $d_6$  as a solvent.  $^1\text{H}$  and  $^{13}\text{C}$  chemical shift were referred to TMS internal standard. The  $^{15}\text{N}$  spectra were referenced to nitromethane, the  $^{31}\text{P}$  spectra to trimethylphosphate. IR spectra were measured on a Vertex 70 (Bruker) spectrometer using a diamond attachment of total internal reflection Platinum ATP.

UV/vis spectra were recorded on a Varian Cary 5000 UV-Vis-NIR spectrophotometer. Microanalysis on C, H and N was performed on a Perkin-Elmer 240C Analyzer.

### 3.3. Synthesis

4-Aminobenzyl(triphenyl)phosphonium bromide has been obtained by a method previously described in the literature [23]. 5-hydroxy-3-methyl-1-phenyl-4-formylpyrazole has been synthesized by the Vilsmeier–Haack reaction between 1-phenyl-3-methyl-2-pyrazolin-5-one, DMF and POCl<sub>3</sub> [24].

*(4-(((3-methyl-5-oxo-1-phenyl-1,5-dihydro-4H-pyrazol-4-ylidene)methyl)amino)benzyl)-triphenylphosphonium bromide (HLBr)*

The **HLBr** was prepared by refluxing an ethanolic solution (10 ml) of 4-aminobenzyl(triphenyl)phosphonium bromide (0.5 g, 12 mmol) and 5-hydroxy-3-methyl-1-phenyl-4-formylpyrazole (0.25 g, 12 mmol) for 4 h. The solution was evaporated to a fifth of the initial volume followed by the addition of tenfold excess of ethyl acetate. The precipitate was separated and recrystallized from a mixture of chloroform/ethyl acetate (1 : 3). Melting point 255 °C. Found C, 68.70; H, 5.10; N, 6.50 %. C<sub>36</sub>H<sub>31</sub>BrN<sub>3</sub>OP Calculated C, 68.36; H, 4.94; N, 6.64 %. Yield 85 %. IR spectrum (cm<sup>-1</sup>): 3300-3450 (br), 2975-3105 (w), 2885 (w), 2857 (w), 1650 (s), 1623 (m), 1596 (m), 1488 (m), 1440 (m), 1291 (s), 1113 (m, broadened). Atom numbering used in NMR description is shown on Scheme 1. For simplicity, the protons of phenyl groups are not numbered and designated as position and fragment name, for example, *o*-NPh means *ortho*-protons of N-phenyl group in pyrazolone moiety, *p*-PPh – *para* protons of the phenyl

substituents in triphenylphosphonium group.  $^1\text{H}$  NMR: (600 MHz, DMSO- $d_6$ ,  $\delta/\text{ppm}$ ) 2.25 (s, 3H,  $\text{H}^6$ ), 5.20 (d, 2H,  $\text{H}^{13}$ ,  $^2J_{\text{PH}} = 15.4$  Hz), 7.02 (dd, 2H,  $\text{H}^{11}$ ,  $^3J_{\text{HH}} = 8.7$ ,  $^4J_{\text{PH}} = 2.54$  Hz), 7.11 (t, 1H,  $p\text{-NPh}$ ,  $^3J = 7.4$  Hz), 7.37 (dd, 2H,  $m\text{-NPh}$ ,  $^3J_{\text{HH}} = 7.4$ ,  $^3J_{\text{HH}} = 8.6$  Hz), 7.45 (d, 2H,  $\text{H}^{10}$ ,  $^3J_{\text{HH}} = 8.7$  Hz), 7.71-7.66 (m, 6H,  $o\text{-PPh}$ ), 7.79-7.73 (m, 6H,  $m\text{-PPh}$ ), 7.93-7.88 (m, 3H,  $p\text{-PPh}$ ), 7.95 (d, 2H,  $o\text{-NPh}$ ,  $^3J_{\text{HH}} = 8.6$  Hz), 8.51 (bs, 1H,  $\text{H}^7$ ), 11.22 (bs, NH).

$^{13}\text{C}$  NMR (151 MHz, DMSO- $d_6$ ,  $\delta/\text{ppm}$ ) 164.7 (s,  $\text{C}^5$ ), 149.0 (s,  $\text{C}^3$ ), 145.2 (s,  $\text{C}^7$ ), 138.9 (s,  $i\text{-NPh}$ ), 138.7 (d,  $\text{C}^9$ ,  $^5J_{\text{PC}} = 4.0$  Hz), 135.1 (d,  $p\text{-PPh}$ ,  $^4J_{\text{PC}} = 3.0$  Hz), 134.0 (d,  $o\text{-PPh}$ ,  $^2J_{\text{PC}} = 9.9$  Hz), 131.9 (d,  $\text{C}^{11}$ ,  $^3J_{\text{PC}} = 5.6$  Hz), 130.1 (d,  $m\text{-PPh}$ ,  $^3J_{\text{PC}} = 12.4$  Hz), 128.7 (s,  $m\text{-NPh}$ ), 124.3 (d,  $\text{C}^{12}$ ,  $^2J_{\text{PC}} = 8.8$  Hz), 123.8 (s,  $p\text{-NPh}$ ), 117.9 (d,  $\text{C}^{10}$ ,  $^4J_{\text{PC}} = 3.3$  Hz), 117.7 (d,  $i\text{-PPh}$ ,  $^1J_{\text{PC}} = 85.5$  Hz), 117.5 (s,  $o\text{-NPh}$ ), 102.2 (s,  $\text{C}^4$ ), 27.8 (d,  $\text{C}^{13}$ ,  $^1J_{\text{PC}} = 46.5$  Hz), 12.6 (s,  $\text{C}^6$ ).  $^{15}\text{N}$  NMR (60 MHz, DMSO- $d_6$ ,  $\delta/\text{ppm}$ ): -92.4 (s,  $\text{N}^2$ ), -190.9 (s,  $\text{N}^1$ ), -252.5 (s,  $\text{N}^8$ ).  $^{31}\text{P}$  NMR (243 MHz, DMSO- $d_6$ ,  $\delta/\text{ppm}$ ): 44.2 (s).

### 3.4. Quantum-chemical calculations

The calculations of electronic and spatial structure of tautomers were carried out within density functional theory (DFT). The hybrid exchange-correlation B3LYP functional [25] with an exchange part in the form suggested by Becke [26] and Lee-Yang-Parr on the correlation part [27] were utilized. The standard extended 6-311G(d,p) split-valence basis set was employed. The structure of the molecules under consideration was optimized without any symmetry restrictions. All stationary points on the potential energy surface were characterized by normal vibration analysis. The Gaussian'03 program [28] was used for calculations. ChemCraft program [29] was

used for the data preparation and visualization of the results. 40 singlet–singlet electronic excitations were simulated for modelling of the UV/vis spectra within the TDDFT method [30, 31]. The influence of the media (ethanolic solution) was taken into account using the polarizable continuum model (PCM) [32, 33] with the standard parameters as implemented in Gaussian'03 program. The IR spectrum was modelled within harmonic oscillator approximation at the same level of theory (B3LYP/6-311G(d,p)), calculated frequencies of fundamental vibrations were scaled by 0.967 as recommended in [34].

#### 4. Conclusions

The phosphonium salt (**HLBr**) was obtained in the reaction of 4-aminobenzyl(triphenyl)phosphonium bromide and 5-hydroxy-3-methyl-1-phenyl-4-formylpyrazole. The existence of pyrazolone isomeric form of **HL**<sup>+</sup> in DMSO solution and solid phase observed from its NMR and IR spectra was further supported by DFT calculations. The results of quantum chemical modelling showed that the activation energy of 5-hydroxypyrazole form of **HL**<sup>+</sup> conversion to pyrazolone-5 one through 1-5 proton sigmatropic shift is 2.68 kcal/mol. Bands in experimental UV/vis spectra for molecular and deprotonated forms of **HL**<sup>+</sup> are in a satisfactory agreement with the results of quantum-chemical calculations. This compound will be further used for synthesis of d-metal coordination compounds.

#### Acknowledgments

This work was supported by the RA MES SCS, within the frames of the «RA MES SCS – YSU-RF SFEDU» joint project No. VnGr-07/2017-35, Ministry of Education, Science and

Technological development of the Republic of Serbia (Grant OI 172055) and taking advantage of the facilities of Resource Centers of SFEDU (“Molecular spectroscopy”, “High-productive calculations” and “Nanoscale structure of matter”).

## References

1. Keglevich, G.; Grün, A.; Hermeecz, I.; Odinet, I. L. *Curr. Org. Chem.* **2011**, 15, 3824–3848.
2. Huang, X.; Weiss, R. G. *Langmuir.* **2006**, 22, 8542–8552.
3. Abdallah, D. J.; Robertson, A.; Hsu, H.-F.; Weiss, R. G. *J. Am. Chem. Soc.* **2000**, 122, 3053–3062.
4. Kagan, V. E.; Wipf, P.; Stoyanovsky, D.; Greenberger, J. S.; Borisenko, G.; Belikova, N.A.; Yanamala, N.; Arias, A. K. S.; Tungekar, M. A.; Jiang, J.; Tyurina, Y. Y.; Ji, J.; Klein-Seetharaman, J.; Pitt, B. R.; Shvedova, A. A.; Bayır, H. *Adv. Drug Deliv. Rev.* **2009**, 61, 1375–1385.
5. Kim, D.-Y.; Min, J.-J. *Nucl. Med. Mol. Imaging.* **2016**, 50, 185–195.
6. Cai, X.; Zhang, J.; Ouyang, Y.; Ma, D.; Tan, S.; Peng, Y. *Langmuir.* **2013**, 29, 5279–5285.
7. Werner, T. *Adv. Synth. Catal.* **2009**, 351, 1469–1481.
8. Kvitko, I. Ya.; Alam, L. V.; Bobrovnikov, M. N.; Avetikiyan, G. B.; Panasiyk, S. L. *Russ. J. Gen. Chem.* **1994**, 64, 657.
9. Amarasekara, A. S.; Owereh, O. S.; Lysenko, K. A.; Timofeeva, T. V. *J. Struct. Chem.* **2009**, 50, 1159–1165.
10. Zhu, H.; Shi, J.; Wei, Z.; Bai, Y.; Bu, L. *Acta Crystallogr.* **2010**, E66, o1583.
11. Jadeja, R. N.; Shah, J. R.; Suresh, E.; Paul, P. *Polyhedron.* **2004**, 23, 2465–2474.

12. Jadeja, R. N.; Shirsat, R. N.; Suresh, E. *Struct. Chem.*, **2005**, 16, 515–520.
13. Thaker, B. T.; Surati, K. R.; Oswal, S.; Jadeja, R. N.; Gupta, V. K. *Struct. Chem.* **2007**, 18, 295–310.
14. Garnovskii, A. D.; Nivorozhkin, A. L.; Minkin, V. I. *Coord. Chem. Rev.* **1993**, 126, 1–69.
15. Syamal, A.; Maurya, M. R. *Coord. Chem. Rev.* **1989**, 95, 183–238.
16. Calligaris, M.; Randaccio, L.; Wilkinson, G. *Comprehensive coordination chemistry*, Vol 2, Pergamon Press: Oxford, 1987.
17. Yamada, S.; Takeuchi, A. *Coord. Chem. Rev.* **1982**, 43, 187–204.
18. Daul, C.; Schlapfer, C.W.; Zelewsky, A. *Struct. Bonding.* **1979**, 36, 129–171.
19. Maslen, H. S.; Waters, T-N. *Coord. Chem. Rev.* **1975**, 17, 137–176.
20. Vigato, P.A.; Tamburini, S. *Coord. Chem. Rev.* **2004**, 248, 1717–2128.
21. Popov, L. D.; Borodkin, S. A.; Scherbakov, I. N.; Tkachenko, Yu. N.; Aleksandrov, G. G.; Beloborodov, S. S.; Zubenko, A. A.; Kogan, V. A.; Maevskii, O. V. *Russ. J. Gen. Chem.* **2013**, 83, 1376.
22. A. Amarasekara, O. Owereh, K. Lyssenko, T. Timofeeva, *J. Struct. Chem.*, **2009**, 50, 1159-1165.
23. Le Corre, M.; Hercouet, A.; Le Stanc, Y.; Le Baron, H. *Tetrahedron*, **1985**, 41, 5313–5320.
24. Wallace, D. J.; Straley, J. M. *J. Org. Chem.*, **1961**, 26, 3825–3826.
25. Stephens, P. J.; Devlin, F. J.; Chabalowski, C. F.; Frisch, M. J. *J. Phys. Chem.* **1994**, 98, 11623–11627.
26. Becke, A. D.; *J. Chem. Phys.* **1993**, 98, 5648–5652.

27. Lee, C.; Yang, W.; Parr, R. G. *Phys. Rev. B.*, **1988**, 37, 785–789.
28. Frisch, M. J.; Trucks, G. W.; Schlegel, H. B.; Scuseria, G. E.; Robb, M. A.; Cheeseman, J. R.; Montgomery, J. A.; Vreven, Jr. T.; Kudin, K. N.; Burant, J. C.; Millam, J. M.; Iyengar, S.S.; Tomasi, J.; Barone, V.; Mennucci, B.; Cossi, M.; Scalmani, G.; Rega, N.; Petersson, G. A.; Nakatsuji, H.; Hada, M.; Ehara, M.; Toyota, K.; Fukuda, R.; Hasegawa, J.; Ishida, M.; Nakajima, T.; Honda, Y.; Kitao, O.; Nakai, H.; Klene, M.; Li, X.; Knox, J. E.; Hratchian, H. P.; Cross, J. B.; Bakken, V.; Adamo, C.; Jaramillo, J.; Gomperts, R.; Stratmann, R.E.; Yazyev, O.; Austin, A.J.; Cammi, R.; Pomelli, C.; Ochterski, J. W.; Ayala, P.Y.; Morokuma, K.; Voth, G. A.; Salvador, P.; Dannenberg, J. J.; Zakrzewski, V.G.; Dapprich, S.; Daniels, A. D.; Strain, M. C.; Farkas, O.; Malick, D. K.; Rabuck, A. D.; Raghavachari, K.; Foresman, J.B.; Ortiz, J.V.; Cui Piskorz, Q.; Komaromi, I.; Martin, R. L.; Fox, D. J.; Keith, T.; Al-Laham, M. A.; Peng, C.Y.; Nanayakkara, A.; Challacombe, M.; Gill, P. M. W.; Johnson, B.; Chen, W.; Wong, M. W.; Gonzalez, C.; Pople, J. A. Gaussian 03, Revision D.01. Gaussian, Inc., Wallingford CT, 2004.
29. Zhurko, G. A.; Zhurko, D. A. Chemcraft Version 1.6 (build 338); <http://www.chemcraftprog.com>.
30. Wang, Y.-G. *J. Phys. Chem. A.* **2009**, 113, 10867–10872.
31. Furche, F.; Rappoport, D. *Theoretical and Computational Chemistry*, Elsevier, 2005, Vol. 16, p. 93.
32. Miertus, S.; Scrocco, E.; Tomasi, J. *Chem. Phys.* **1981**, 55, 117–129.
33. Cammi, R.; Tomasi, J. *J. Comput. Chem.* **1995**, 16, 1449–1458.

34. NIST Computational Chemistry Comparison and Benchmark Database; NIST Standard Reference Database Number 101, Release 18, October 2016, Editor: Russell D. Johnson III  
<http://cccbdb.nist.gov/>